Compensation of Model Errors in Electrocardiographic Imaging Using Bayesian Estimation

Furkan Aldemir, Yesim Serinagaoglu Dogrusoz

Electrical and Electronics Engineering Department,
Middle East Technical University, Ankara, Turkey

Abstract

Bayesian Maximum a Posteriori (MAP) estimation has been successfully applied to electrocardiographic imaging (ECGI). However, in most studies, MAP deals only with the measurement noise and ignores the forward model errors. In this study, we incorporated model uncertainty in the MAP formulation to improve the inverse reconstructions. Measured electrograms (EGM) from the University of Utah were used to form training and test datasets. Body surface potential (BSP) measurements were simulated at 30 dB SNR. The inverse problem was solved using MAP estimation. The training dataset was used to define the prior probability function (pdf). Both the measurement noise and model error were assumed to be uncorrelated with the EGMs. Model error was introduced as shift in the heart position and scaling of the heart size. Three model error pdfs were considered: no compensation (model error is assumed as zero in the solution); model error is modeled as independent and identically distributed (IID) and correlated across leads (CORR). For IID and CORR, pdf was estimated based on all geometry disturbances. Results were evaluated using spatial (sCC) and temporal (tCC) correlation coefficients. These results showed that including model errors in the MAP formulation, even in a simple form such as the IID, improved the reconstructions over ignoring them.

1. Introduction

Noninvasive ECGI is a promising clinical tool for detecting arrhythmias and mapping arrhythmic substrates [1]. It uses body surface potential (BSP) measurements and a patient-specific mathematical model of the torso to obtain the electrical activity of the heart. However, due to smoothing and attenuation of the cardiac signals within the torso, this inverse problem is an ill-posed problem, and regularization is needed to obtain an accurate solution.

Statistical estimation methods have been applied to ECGI successfully when adequate *a priori* information is available [2–5]. Bayesian Maximum a Posteriori (MAP) estimation is among these well-known estimation methods. In this method, the posterior probability density (pdf) of the electrograms (EGM) is computed using the likelihood function of the BSPs and a prior pdf of the EGM. The EGMs maximizing this posterior pdf is the MAP solution. In literature, the effects of measurement noise are well studied, and the pdf of this noise is incorporated in the solution procedure [4, 5]. However, errors in the mathematical (forward) model, which arise from uncertainties in the heart and torso geometries, electrode positions, and conductivity distribution within the torso, are usually not taken into account.

In an earlier study, we defined the perturbations due to these geometric errors as an additional noise term to the measurement noise for improving the Kalman filter-based ECGI reconstructions [5]. We proposed methods for estimating the variance for this simple noise model. In this study, our aim is to study the effects of scaling and shifting errors in the heart model on the MAP-based ECGI performance, and investigate how these errors can be taken into account in the inverse formulation to achieve a more robust solution.

2. Problem Definition

The relationship between the EGM and BSP in ECGI can be explained through the following equation:

$$y = Ax + n, \tag{1}$$

where $y \in \mathbb{R}^{\mathbb{M}}$ and $x \in \mathbb{R}^{\mathbb{N}}$ are the BSP measurements and EGM, respectively, $n \in \mathbb{R}^{\mathbb{M}}$ is the measurement noise, and $A \in \mathbb{R}^{\mathbb{M}\times\mathbb{N}}$ is the forward transfer matrix, which reflects the properties of the true torso-heart geometry. However, perturbations in the geometric model or conductivity values used in the forward computations introduce an error in this forward matrix. If we take this error into account, the model used for the inverse computations becomes:

$$y = (\tilde{A} + A_{err})x + n, \tag{2}$$

 ISSN: 2325-887X DOI: 10.22489/CinC.2021.227

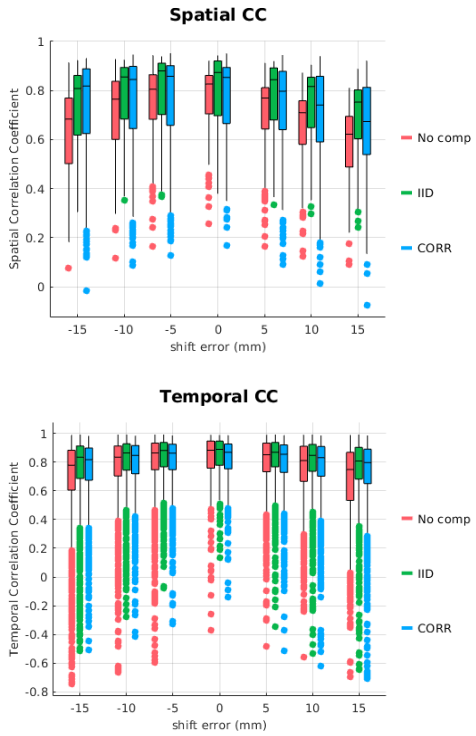

Figure 1: sCC and tCC boxplots for the shift errors.

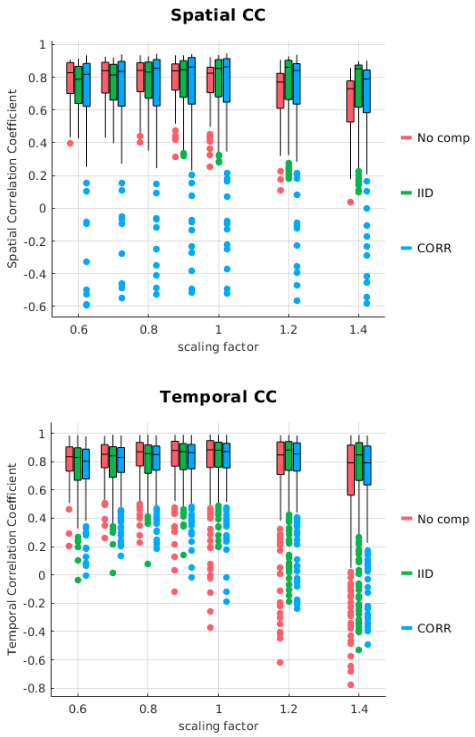

Figure 2: sCC and tCC boxplots for the scaling errors.

where $\tilde{A}$ is the forward matrix corresponding to the incorrect geometry, and A_{err} is its deviation from the true matrix A. Eqn. 1 can be modified to include a new geometric error term $\epsilon = A_{err}x$ as:

$$y = \tilde{A}x + \epsilon + n, \tag{3}$$

which allows the introduction of a more general noise term:

$$\tilde{n} = \epsilon + n. \tag{4}$$

2.1. Bayesian MAP Estimation

Bayesian MAP estimation maximizes the following posterior pdf of x, which can be expressed in terms of the likelihood function $p(y\backslash x)$ and an a priori pdf $p(x)$ of EGMs:

$$p(x\backslash y) = \frac{p(y\backslash x)p(x)}{p(y)} \tag{5}$$

If we assume that x and y are jointly Gaussian, $x \sim N(\bar{x}, C_x)$, $\tilde{n} \sim N(0, C_{\tilde{n}})$, then the MAP estimate of x becomes:

$$\hat{x} = (\tilde{A}^T C_{\tilde{n}}^{-1} \tilde{A} + C_x^{-1})^{-1} (\tilde{A}^T C_{\tilde{n}}^{-1} y + C_x^{-1} \bar{x}) \tag{6}$$

Note that ϵ is correlated with the EGMs, however in this initial study, we ignore this correlation for simplicity of the model. We assume that ϵ and n are uncorrelated with x and with each other. The measurement noise was taken to be independent and identically distributed (iid) with $n \sim N(0, \sigma_n^2 I)$ and $\epsilon \sim N(0, C_\epsilon)$, resulting in $C_{\tilde{n}} = C_\epsilon + \sigma_n^2 I$.

3. Datasets

The data used in this study came from experiments carried out at the University of Utah, Nora Eccles Harrison Cardiovascular Research and Training Institute (CVRTI) [6]. In these experiments, an excised dog heart, perfused by a support dog's circulatory system, was suspended in an adolescent torso-shaped tank. The heart was ventricularly paced from the epicardial surface, and EGMs were recorded via 490-lead sock electrodes (1000 Hz sampling rate). BSPs were simulated by multiplying the EGMs by a forward matrix and then adding normally distributed noise at 30 dB SNR. This forward matrix was computed by using the boundary element method (BEM) with lungs included in the geometric model. The fine torso geometry consisted of 771 nodes. BSPs corresponding to 192 electrode locations were subsampled and used in ECGI.

This study is our first attempt to incorporate a geometric error component in the MAP formulation. Thus, currently we used a single ventricularly paced beat (QRS region, $\sim$ 100 ms duration) as the test beat. The corresponding BSPs

Table 1: Spatial correlation coefficients of the reconstructed EGMs. Shift error includes x, y and z shifts..

Error	No comp	IID	CORR
scale			
0.6	0.83 (0.19)	0.79 (0.23)	0.82 (0.26)
0.7	0.84 (0.19)	0.81 (0.22)	0.84 (0.27)
0.8	0.84 (0.18)	0.83 (0.22)	0.85 (0.28)
0.9	0.84 (0.16)	0.85 (0.22)	0.86 (0.28)
1.0	0.83 (0.15)	0.85 (0.23)	0.86 (0.26)
1.2	0.77 (0.21)	0.86 (0.24)	0.84 (0.25)
1.4	0.73 (0.25)	0.85 (0.26)	0.79 (0.26)
shift (mm)			
-15	0.68 (0.27)	0.81 (0.24)	0.82 (0.26)
-10	0.76 (0.24)	0.85 (0.21)	0.84 (0.25)
-6	0.80 (0.18)	0.88 (0.21)	0.86 (0.24)
0	0.83 (0.16)	0.87 (0.22)	0.85 (0.23)
6	0.77 (0.17)	0.84 (0.21)	0.80 (0.24)
10	0.71 (0.18)	0.82 (0.21)	0.74 (0.27)
15	0.62 (0.21)	0.75 (0.20)	0.67 (0.27)

were obtained using a forward matrix computed for the true geometry. The EGMs in the training set were also ventricularly paced beats, with pacing locations within the third order neighbourhood of the test beat pacing site [7]. The prior pdf model parameters $\bar{x}$ and C_x were estimated from these training EGMs, $X_{tr} \in \mathbb{R}^{\mathbb{N}\times\mathbb{T}}$.

4. Geometric Error Model Scenarios

We introduced the geometric error as shift and scaling errors in the heart geometry [5]: (1) The heart position was shifted by -15 to 15 mm along each axis (separately). For the second scenario, the size of the heart was modified by a scaling factor of 0.6 to 1.4. 0 shift and 1.0 scaling factor correspond to no geometric error. For each geometric error scenario, a new forward matrix $\tilde{A}$ was computed using the BEM approach for a homogeneous torso, which is used to solve the inverse problem for the test beat.

C_ϵ was estimated using "error training data" composed of all corresponding A_{err} matrices and X_{tr}:

$$E_{tr} = [A_{err,1}X_{tr} \ \ldots \ A_{err,k}X_{tr}], \qquad (7)$$

where $A_{err,i}$, $i = 1,\ldots,k$, is the error in the forward model for either each shift or each scale amount. Note that two separate E_{tr} matrices were obtained; one for the shift and the other for the scaling errors. Each of these E_{tr} matrices were then used to define two different C_ϵ estimates: (1) IID: ϵ is iid with $C_\epsilon = \sigma_\epsilon^2 I$. (2) CORR: there is correlation across leads; C_ϵ is a non-diagonal matrix. Additionally, we solved the inverse problem without compensating for these geometric errors ("No comp") for comparison. For this case, ϵ is assumed to be zero, and hence $C_\epsilon = 0$.

Table 2: Temporal correlation coefficients of reconstructed EGMs. Shift error includes x, y and z shifts.

Error	No comp	IID	CORR
scale			
0.6	0.83 (0.17)	0.83 (0.23)	0.80 (0.21)
0.7	0.85 (0.16)	0.84 (0.22)	0.83 (0.17)
0.8	0.87 (0.17)	0.86 (0.20)	0.85 (0.17)
0.9	0.88 (0.18)	0.87 (0.19)	0.87 (0.17)
1.0	0.88 (0.19)	0.88 (0.18)	0.87 (0.18)
1.2	0.85 (0.23)	0.88 (0.20)	0.86 (0.20)
1.4	0.79 (0.36)	0.85 (0.27)	0.79 (0.28)
shift (mm)			
-15	0.78 (0.28)	0.84 (0.23)	0.82 (0.22)
-10	0.84 (0.21)	0.87 (0.18)	0.85 (0.20)
-6	0.87 (0.19)	0.88 (0.17)	0.86 (0.18)
0	0.88 (0.19)	0.89 (0.17)	0.87 (0.17)
6	0.85 (0.20)	0.87 (0.17)	0.86 (0.19)
10	0.81 (0.24)	0.85 (0.19)	0.83 (0.21)
15	0.75 (0.34)	0.81 (0.22)	0.80 (0.24)

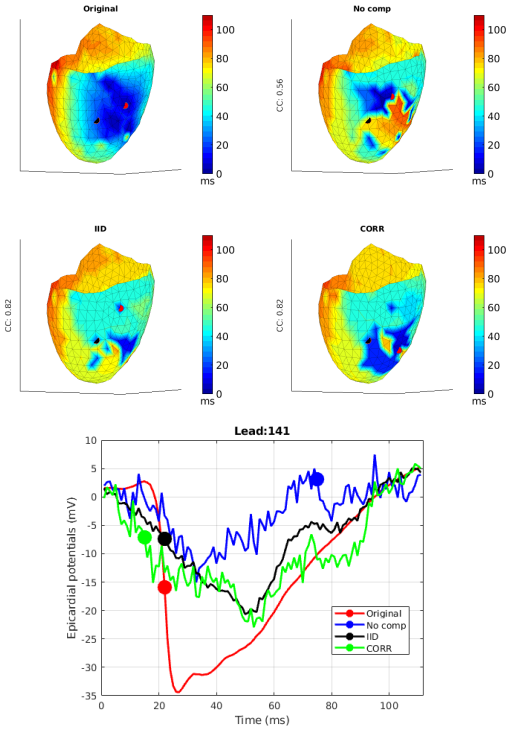

Figure 3: Top: Ground truth and reconstructed activation time (AT) maps for shift error of -15 mm in the z-axis, Bottom: EGMs at lead 141 (black dot on the AT maps); with the corresponding AT marked with a dot of the same color.

5. Results

Inverse reconstructions were obtained for each shift and scale geometric error case, using the corresponding $\tilde{A}$ ma-

trix and the geometric error compensation method. Reconstructed EGMs were compared with the measured EGMs using temporal and spatial correlation coefficients (tCC and sCC). Activation times (AT) were also computed by the spatio-temporal method proposed in [8]. Solution ATs were compared with the ground truth ATs qualitatively and by using Pearson's correlation.

Figures 1 and 2, along with Tables 1 and Table 2, display the sCC and tCC values and show how the compensation method performs against no compensation for the shifting and scaling error cases. For the shifting error case, values corresponding to the three directions, x, y and z, are combined together. The values in the Tables 1-2 are median values, with the interquartile range (IQR - the difference between the first and third quartiles) in indicated parentheses. Median sCC values increased up to 21.0% with IID and 20.6% with CORR compared to "no comp". Meanwhile, median tCC values were mostly comparable but increased up to 8.0% with IID and 6.7% with CORR in some cases. Greater improvements were generally observed for larger shift errors. For the scaling error, "no comp" results suffered more for increasing the heart size than decreasing it. Both IID & CORR improved the reconstructions.

Figure 3 shows the ground truth & reconstructed AT maps for a shift error of -15 mm along the z-axis, and the true and reconstructed EGMs corresponding to one lead. Both IID and CORR AT maps were substantially improved over the 'No comp' case. The CC for AT increased by 46% from 0.56 ('No comp') to 0.82 (IID, CORR) Pacing sites were estimated from these AT maps as the earliest activated node, and indicated as red dots on the AT maps. Despite the improvements in the AT maps with the proposed methods, none of the reconstructions had the same AT wavefront pattern as the ground truth. Consequently, pacing site localization was not reliable. Both IID and CORR resulted in EGM reconstructions with better fidelity to the ground truth. 'No comp' and CORR resulted in noisy EGM estimates, but IID reconstruction was smoother, which in turn improves the AT estimation accuracy.

6. Discussion and Conclusion

In this preliminary study with limited test and training data, we showed that including model errors in the MAP formulation, even in a simple form such as the IID, improved the reconstructions over ignoring them. However, these results should be further investigated with a larger experimental dataset with diverse geometric error sources. The geometric error here was assumed to be independent of EGMs, which in fact is an overly simplified and unrealistic assumption. We are currently extending our work to include correlation between the geometric error term ($\epsilon = A_{err}x$) and the EGMs. Training set for this study came from the same dog heart as the test beat. We are working on different training scenarios, which utilize simulated datasets.

Acknowledgments

This work was supported by The Scientific and Technological Research Council of Turkey, grant number 118E244. The authors would like to thank Dr. Robert S. MacLeod for the data used in this study.

References

[1] Cluitmans MJM, Peeters RLM, Westra RL, Volders PGA. Noninvasive reconstruction of cardiac electrical activity: update on current methods, applications and challenges. Netherlands Heart Journal 2015;23(6):301–311.

[2] Erenler T, Dogrusoz YS. ML and MAP estimation of parameters for the Kalman filter and smoother applied to electrocardiographic imaging. Med Biol Eng Comp 2019; 57(10):2093–2113.

[3] van Oosterom A. The use of the spatial covariance in computing pericardial potentials. IEEE Trans on Biomed Eng 1999;46(7):778–787.

[4] Serinagaoglu Y, Brooks DH, MacLeod RS. Improved performance of bayesian solutions for inverse electrocardiography using multiple information sources. IEEE Trans on Biomed Eng 2006;53(10):2024–2034.

[5] Aydin U, Dogrusoz YS. A Kalman filter-based approach to reduce the effects of geometric errors and the measurement noise in the inverse ecg problem. Med Biol Eng Comp 2011; 49(9):1003–1013.

[6] MacLeod R, Taccardi B, Lux R. Electrocardiographic mapping in a realistic torso tank preparation. In Proc. of 17th Int. Conf. of the IEEE EMBS, volume 1. 1995; 245–246 vol.1.

[7] Ozkoc E, Sunger E, Ugurlu K, Dogrusoz YS. Prior model selection in Bayesian MAP estimation-based ecg reconstruction. In 2021 13th Int. Conf. on Meas. Bratislava: IEEE, 2021; 142–145.

[8] Erem B, Coll-Font J, Orellana R, Stovicek P, Brooks D. Using transmural regularization and dynamic modeling for noninvasive cardiac potential imaging of endocardial pacing with imprecise thoracic geometry. IEEE Trans on Med Imag 03 2014;33:726–38.

Address for correspondence:

Furkan Aldemir
Electrical and Electronics Engineering Department
Middle East Technical University, Ankara, Turkey
furkan.aldemir@metu.edu.tr